

CONF-9502109--1

To be submitted for Proceedings on International Symposium on Gamma Titanium Aluminides (ISGTA'95),
February 12-16, 1995, Las Vegas, NV.

TIME-DEPENDENT STRESS CONCENTRATION AND MICROCRACK NUCLEATION IN TiAl†

M. H. Yoo*

Metals and Ceramics Division
Oak Ridge National Laboratory
Oak Ridge, TN 37831-6115

The submitted manuscript has been
authored by a contractor of the U.S.
Government under contract No. DE-
AC05-84OR21400. Accordingly, the U.S.
Government retains a nonexclusive,
royalty-free license to publish or reproduce
the published form of this contribution, or
allow others to do so, for U.S. Government
purposes.

Abstract

Localized stress evolution associated with the interaction of slip or twinning with an interface is treated by means of a superposition of the "internal loading" of a crystalline subsystem by dynamic dislocation pile-up and the stress relaxation by climb of interfacial dislocations. The peak value of a stress concentration factor depends on both the angular function that includes the effect of mode mixity and the ratio of characteristic times for stress relaxation and internal loading. The available experimental data on orientation and strain-rate dependences of interfacial fracture mode in polysynthetically twinned TiAl crystals are discussed in view of the theoretical concepts presented in this paper.

DISCLAIMER

This report was prepared as an account of work sponsored by an agency of the United States Government. Neither the United States Government nor any agency thereof, nor any of their employees, makes any warranty, express or implied, or assumes any legal liability or responsibility for the accuracy, completeness, or usefulness of any information, apparatus, product, or process disclosed, or represents that its use would not infringe privately owned rights. Reference herein to any specific commercial product, process, or service by trade name, trademark, manufacturer, or otherwise does not necessarily constitute or imply its endorsement, recommendation, or favoring by the United States Government or any agency thereof. The views and opinions of authors expressed herein do not necessarily state or reflect those of the United States Government or any agency thereof.

†Research sponsored by the Division of Materials Sciences, U. S. Department of Energy, under contract DE-AC05-84OR21400 with Martin Marietta Energy Systems, Inc. and in part by Alexander von Humboldt Foundation, Germany

*Work performed during his foreign assignment to Max-Planck-Institut für Eisenforschung, 40074 Düsseldorf, and Technische Universität Hamburg-Harburg, 21073 Hamburg

DISTRIBUTION OF THIS DOCUMENT IS UNLIMITED

JR

MASTER

DISCLAIMER

**Portions of this document may be illegible
in electronic image products. Images are
produced from the best available original
document.**

Introduction

Strength and ductility of two-phase lamellar TiAl alloys depend on deformation characteristics of the constituent phases and intricate interaction between deformation modes and various interfaces. Within the past decade, because of the capability of growing the so-called polysynthetically twinned (PST) crystals [1], there has been a significant advance in understanding the role of interfaces in yield strength and ductility of two-phase TiAl alloys with lamellar microstructures. In addition to γ - α_2 interfaces, a lamellar microstructure of a PST crystal consists of three different types of intervariant γ/γ lamellar interfaces, i.e., (1) true-twin boundaries, (2) pseudo-twin boundaries, and (3) 120° rotational boundaries. All of these boundaries, especially when they are in semicoherent form, can act as sites for slip and/or twin initiation [2]. The role of these lamellar boundaries as dislocation sources may be partly responsible for the measurable ductility reported in two-phase lamellar TiAl alloys as compared to single-phase γ -TiAl alloys [3,4].

When a dislocation pile-up occurs against such an interface, as well as a high-angle grain boundary, stress concentration at the interface may reach a level sufficiently high for either an initiation of a deformation mode into the adjacent grain (or domain) leading to a Hall-Petch type relationship, or a crack nucleation by the Stroh mechanism. Recently, Hazzledine and Kad [5] discussed the orientation dependent yield and fracture stresses reported in PST TiAl crystals [6] in terms of Hall-Petch and Stroh mechanisms. In view of the fact that all the deformation modes in γ -TiAl occur on {111} planes and the ideal cleavage (Griffiths) energy is lowest on these planes, Yoo et al. [7] pointed out the importance of mode-mixity (I-II or I-III) not only in crack-tip plasticity, but also in crack nucleation by stress concentration due to a dislocation pile-up.

Most of modeling analyses for the stress concentration associated with a pile-up of dislocations, including the above two cases [5,7], are based on a static equilibrium condition, and as such these cannot be applied to treat dynamic or quasi-static aspect of a stress concentration. The objective of this paper is to address time dependence of stress concentration associated with a dislocation pile-up in the case of two-phase TiAl alloys, and discuss interfacial structures and properties that control the kinetics of stress relaxation. The change in fracture mode due to the strain-rate difference reported in the PST crystals of a soft orientation [8] is also discussed in terms of the present analysis.

Stress Concentration by a Dislocation Pile-up

Static equilibrium distribution of a dislocation pileup was obtained by use of the concept of continuously distributed dislocations with infinitesimal Burgers vectors [9]. The lattice Burgers vectors to be considered are $1/2<110]$ of ordinary slip, $<101]$ of superlattice slip, $1/2<112]$ of superlattice slip, and $1/6<112]$ of true-twining. When we consider an effective barrier for a dislocation pile-up to be any one of the three types of interfaces mentioned above, a wide variety of critical conditions for localized deformation and microcrack nucleation can be envisaged, as schematically illustrated in Fig. 1. In Figure 1, the parts (a and b) indicate that an interface can be a source and a sink of dislocations, (c) a site for slip transfer, (d or e) for crack nucleation within the grain (or domain) or into the next grain (or domain), and finally (f, g, and h) for microcracking along the interfaces. When the dislocation initiation, absorption, and transfer at interfaces of Fig. 1 (a-c) are prevalent, this localized microplasticity may lead to a relatively large elongation at failure, ϵ_f . On the other hand, when the conditions for crack nucleation of any one type of Fig. 1 (d-h) is satisfied before the localized microplasticity sets in, the propensity of microcracking will be enhanced, thus ending up with a relatively low value of tensile elongation at failure, ϵ_f .

The critical shear stress for microcrack nucleation under the static stress concentration due to a pile-up of either slip or twin dislocations was given earlier [7,10], which includes the effect of elastic anisotropy on dislocation line energy [11].

$$\tau_c = \pi (A/l)^{1/2} [\Gamma/H(\theta)]^{1/2}, \quad (1)$$

where $A=Kb/2\pi$, K the energy factor, b the magnitude of Burgers vector \mathbf{b} , l the pile-up length, and Γ is the anisotropic surface energy. The dependence of stress concentration on the angle, θ , as defined in Fig. 1 is given by

$$H(\theta) = (\rho_e f_I)^2 + (\rho_s f_{II})^2 + (\rho_s f_{III})^2, \quad (2)$$

where $\rho_e = K_e \sin^2 \beta / K$, $\rho_s = K_s \cos^2 \beta / K$, and β is the angle between \mathbf{b} and the dislocation line direction. The subscripts denote edge and screw components. The angular functions (f_I , f_{II} , and f_{III}) are identical to those of the elastic stress field of a crack tip, which have the well-known analytic forms for the case of elastic isotropy [12]. Effects of elastic anisotropy on these angular functions were discussed earlier for TiAl [7], but these are neglected in this paper for simplicity. Also neglected is the small tetragonality ($\sim 2\%$) of TiAl with the $L1_0$ structure.

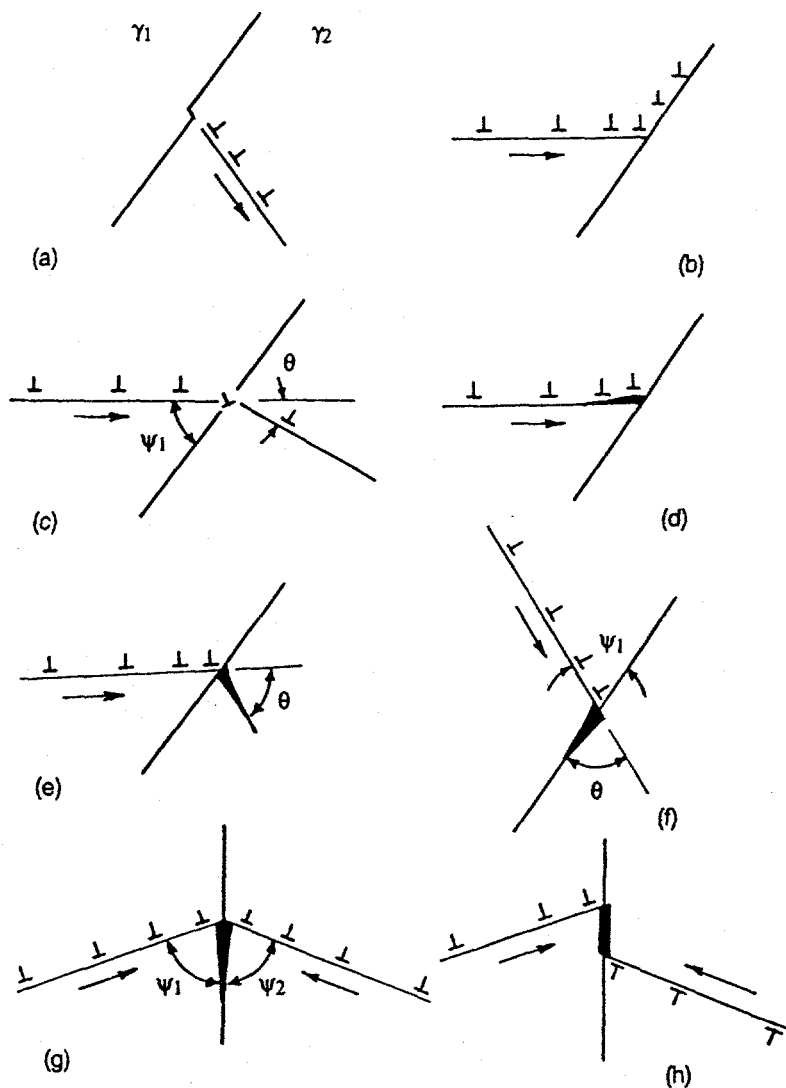


Fig. 1 - Schematic illustrations of dislocation pile-ups against γ_1/γ_2 interfaces.

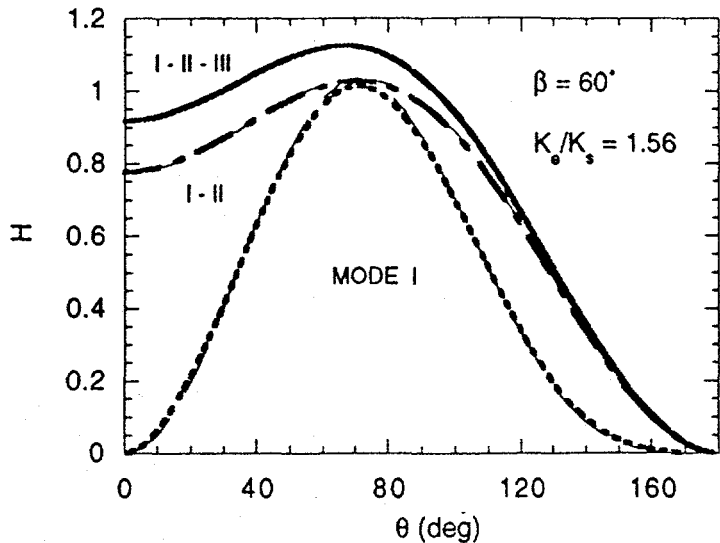


Fig. 2 - Angular dependence of the stress concentration at a (111) twin boundary due to a pile-up of $1/2[110]$ dislocations on the $(\bar{1}11)$ plane.

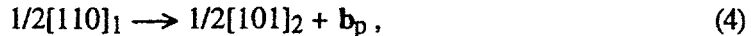
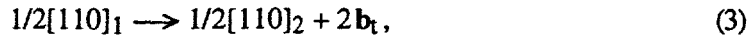
Figure 2 shows the angular term, $H(\theta)$, for the case of a pile-up of straight ($\beta = 60^\circ$) ordinary dislocations of $b = 1/2[110]$ on the $(\bar{1}11)$ slip plane against an (111) interface which can be any one of the three lamellar boundary types. Using the calculated elastic constants of TiAl [15], we obtain the relevant energy factors for this case to be $K = 79.4$, $K_e = 95.2$, and $K_s = 59.9$ in units of GPa. In Fig. 2, while the solid curve gives an overall angular dependence of $H(\theta)$, the two dashed curves show contribution from the edge component, $b_e = 1/4[211]$, giving the maximum of mode-I part at $\theta = 70.5^\circ$ and that of mode-II part at $\theta = 0^\circ$. Contribution from the screw component (mode-III), $b_s = 1/4[01\bar{1}]$, is relatively small as can be discerned from the difference between the top two curves in Fig. 2. The role of mode-II part in lowering τ_c is very important, particularly at low angles (e.g., $\theta < 60^\circ$). This importance of mode mixity in microcrack nucleation at the head of a dislocation pile-up was discussed earlier [7].

The surface energy, Γ , in Eq. (1) is dependent upon crystallographic orientation, not as a continuous function of θ , but discontinuously having sharp low-energy cusps along some low index $\{hkl\}$ planes, e.g., (111) and (100) in TiAl [16]. Therefore, the critical shear stress for a pile-up of ordinary dislocations in γ_1 intersecting an (111) interface along the $[01\bar{1}]$ direction depends on the angular dependence of the ratio, Γ/H , within the adjacent γ_2 domain(or grain) or along the interface [17]. For example, if the interface under consideration is that of a true-twin boundary, then the acute angle between the slip plane and the interface is the same (see Fig. 1), i.e., $\psi_1 = \psi_2 = 70.5^\circ$, which gives $\theta = \pi - 2\psi = 39.0^\circ$ (see Fig. 1(e)). This results in the low (111) surface energy, $\Gamma = \Gamma_{(111)} = 2.25 \text{ J/m}^2$ and $H = 1.05$ for translamellar microcracking in γ_2 . In the case of Fig. 1(f) for interlamellar microcracking, Γ in Eq. (1) should be replaced by $\Gamma = G_c/2$, where the cohesive energy of the interface is $G_c = 2\Gamma_{(111)} - \Gamma_t$ with $\Gamma_t = 60 \text{ mJ/m}^2$ [15]. These give $\Gamma = 2.22 \text{ J/m}^2$ and $H = 1.12$ at $\psi_1 = \theta = 70.5^\circ$. Therefore, as far as the energetic criterion for microcracking at a true-twin interface is concerned, crack nucleation along the interface is slightly more favored (i.e., τ_c is lower by 6%) than cleavage initiation on the $(\bar{1}11)$ plane of γ_2 domain in twinned orientation.

Effective Barriers for a Dislocation Pile-up

When a leading dislocation of the $1/2[110](\bar{1}11)$ ordinary slip system approaches an interface, it is elastically repelled from, or attracted to, the interface depending on the difference in elastic moduli between two phases or an elastic anisotropy effect in the case of a single phase [10,17]. Regardless of the sign of this elastic interaction force, however, the leading dislocation is eventually incorporated into the interface owing to the repulsive forces exerted by the trailing dislocations of the same type.

Two possible dislocation reactions for incorporation of an ordinary dislocation into a true-twin interface are



where the subscripts 1 and 2 denote γ_1 (matrix) and γ_2 (twin), and the resultant partial dislocations created at the interface are either $\mathbf{b}_t = 1/6[112]$ of true-twinning, or $\mathbf{b}_p = 1/6[2\bar{1}\bar{1}]$ for pseudo-twinning. The simple Frank's rule indicates that both reactions are energetically unfavorable because they require an increase in elastic line energies. In the reaction by Eq. (3), $2\mathbf{b}_t$ would decompose spontaneously into two individual true-twinning partials, of which mobility is expected to be high on the (111) coherent twin boundary. Whereas, in the reaction by Eq. (4), the resulting superpartial dislocation, $1/2[101]$, would have to trail an $(\bar{1}11)$ antiphase boundary (APB) until the subsequent incorporation process of the second ordinary dislocation takes place. In addition, if the mobility of pseudo-twinning partials on the twin boundary is lower than that of true-twinning partials, then the first reaction, Eq. (3), is more likely to occur than the second, Eq. (4).

The example described above, involving a coherent true-twin boundary interface, produces resultant partial dislocations with Burgers vectors lying in the interface. In general, however, the interfacial partial dislocations resulting from incorporation process has a Burgers vector pointing in an inclined direction with respect to the interface as schematically shown in Fig. 1 (c). Consequently, in this general case, the dynamic aspect of the stress concentration by a dislocation pile-up against an interface is critically controlled by climb mobility of these interfacial dislocations.

Time-Dependent Stress Concentration

If the stress relaxation by climb of interfacial dislocations is considered as an "interfacial diffusion process," then the earlier solution of an overall evolution of the local normal stress by a linear elasto-diffusion approach [14] may be applicable. It should be emphasized here that the climb process of interfacial dislocations is possible not only by long-range diffusion of constituent Ti and Al atoms at elevated temperatures, but also by localized atomic rearrangement in the interfacial dislocation core structure under the influence of stress concentration even at room temperature. Figure 3 shows a solution obtained earlier [13] with $H = 1$ and $\alpha = 10^6$. The numerical factors involved are defined as follows: $\alpha = t_r/t_l$, $\lambda = l/d$, and $\tau = t/t_l$, where λ is a distance from the barrier normalized to the interspacing (d) of such barriers, τ is a time normalized to the characteristic time for internal loading (t_l) and t_r is the characteristic time for stress relaxation. The peak stress (σ^*), the absolute maximum of $\sigma(\lambda, \tau)$, is $\sigma^*/\sigma_\infty = 0.79 H \alpha^{1/6}$, which occurs at $\tau^* = 2.9$. Here, σ_∞ denotes the far-field applied stress. The peak value of stress concentration factor, σ/σ_∞ , will reach 7.9 when it is assumed that $H = 1$ and $\alpha = 10^6$. For $\sigma^* > 8 \sigma_\infty$, the necessary condition is $\alpha > 10^6$.

The characteristic time for internal loading, t_l , is conceptually easier to assess than that of stress relaxation. At low temperature, $T < 0.4T_m$ (T_m is the melting point), where long-range diffusion is negligible, t_l may be assumed to be inversely proportional to the mobility of

lattice dislocations in a pile-up. Unless the localized microplasticity (see Fig. 1 (a-c)) occurs readily, a relatively small t_f together with a large t_r causes an extremely high value of α . In the meantime, it is physically reasonable to assume that t_f is also inversely proportional to the applied strain rate, $\dot{\epsilon}$. Therefore, the effect of applied strain rate on the peak value of dynamic stress concentration is expected to play an important role at room temperature.

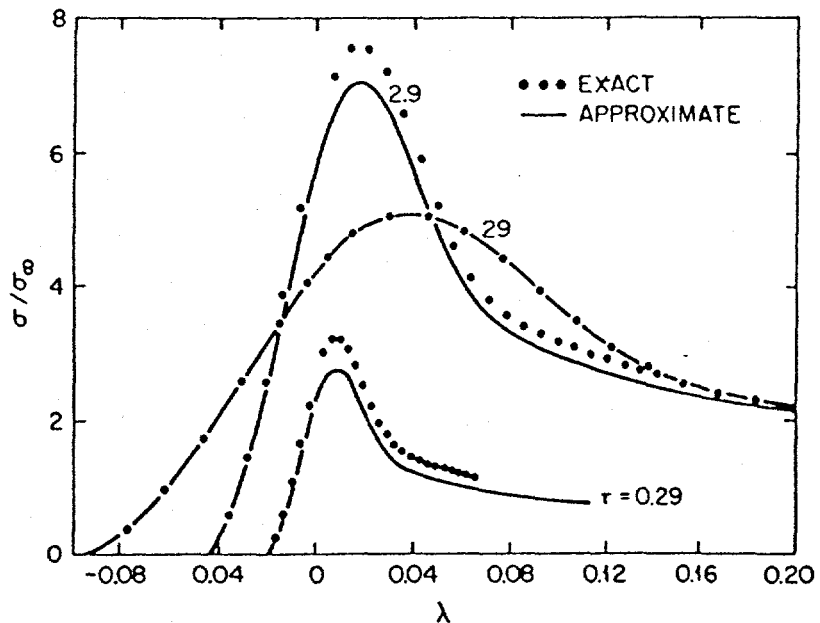


Fig. 3 - Spatial and temporal evolution of the localized normal stress (from Ref. [13]).

Discussion and Summary

Because of the lack of information on mobilities of lattice and interfacial dislocations, quantitative analysis of time-dependent stress concentration and its role in microcrack nucleation in TiAl are difficult to establish. According to the recent atomistic simulation study [18], the 'ideal' friction stress for a <101> superdislocation with the planar core structure is to range from 0.001-0.002 μ (μ is the elastic shear modulus) at 0 K, which depends on the line orientation. The friction stress for a 1/2<110> ordinary dislocation is consistently higher than that for a superdislocation. This difference implies that the α value associated with a pile-up of superdislocations is expected to be higher than that of ordinary dislocations. As for mobility of interfacial dislocations, the *in situ* straining transmission electron microscopy observation by Couret et al. [19] indicates that, in addition to an apparent friction stress at room temperature, the mobility of true-twinning partials is controlled also by pinning of the partials on small 'extrinsic obstacles,' such as Frank dislocations resulting from the interaction between the partial and an ordinary dislocation.

In the remainder of this paper, a discussion of the experimental results by Oh et al. [8] is given in view of the theoretical concepts developed in the sections above. Figure 4 shows a schematic drawing of their results in the case of PST TiAl crystals in a soft ($\phi = 31^\circ$) orientation under the same environmental condition at room temperature. When the applied strain rate in tension was $\dot{\epsilon} = 2 \times 10^{-4} \text{ s}^{-1}$, the fracture mode was an interlamellar type along the (111) γ/γ interfaces parallel to the α_2/γ interfaces, as shown by Fig. 4(a), and the tensile elongation was 16%. When the strain rate was increased to $\dot{\epsilon} = 1 \times 10^{-1} \text{ s}^{-1}$, the fracture mode was changed to a translamellar type (Fig. 4(b)), which occurred with nearly a factor of two increase in ductility of $\epsilon_f = 30\%$.

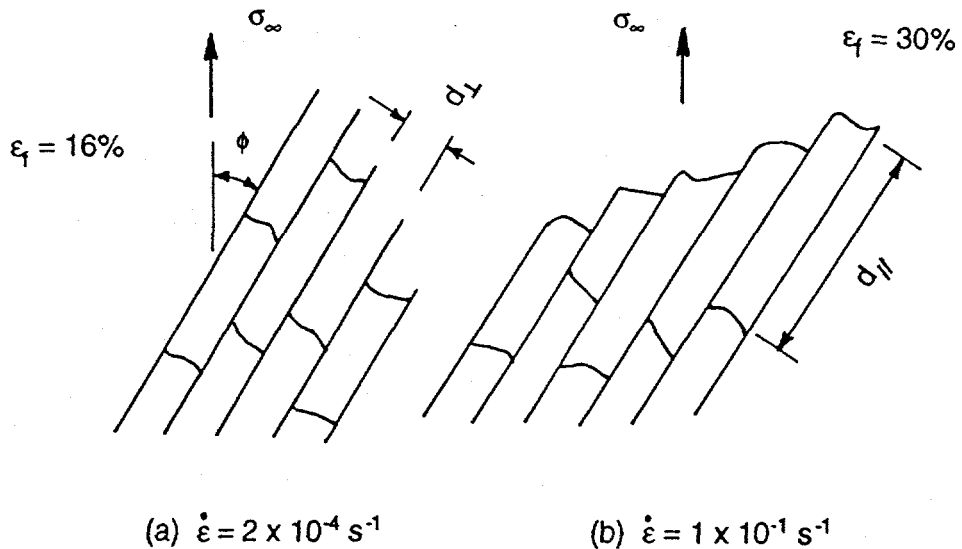


Fig. 4 - Schematic illustrations of the change in fracture mode in PST TiAl crystals of soft orientation ($\phi = 31^\circ$) with two different strain rates under the same environmental condition at room temperature (based on Ref. [8]).

As far as the energetic aspect of cleavage fracture is concerned, the interlamellar cleavage (Fig. 4(a)) may be related to the reduced interfacial energy by hydrogen segregation and the mixed-mode (I-II-III) effect. The change in fracture morphology to a translamellar type that occurred by changing the strain rate to a higher value (Fig. 4(b)) can be rationalized in terms of the kinetic aspect of interfacial crack nucleation and propagation in the following two views: (a) kinetics of hydrogen embrittlement and (b) dynamics of stress concentration. First, the case of Fig. 4(a) is considered to occur simply due to hydrogen embrittlement effect, where segregation and migration of hydrogen atoms along the planar γ/γ interfaces parallel to the α_2/γ interfaces was effected under the low strain rate. This suggests that the case of Fig. 4(b) is the energetically more favorable one, but it did not happen because the applied strain rate was too high for the kinetics of hydrogen embrittlement become important. Second, the additional factor pertaining to the dynamic aspect of stress concentration is that, in Fig. 4(b), the increase in strain rate might have raised α (lower t_f) and the normal stress (σ) to those γ/γ interfaces approximately perpendicular to the lamellar boundary, resulting in the translamellar cleavage. When the strain rate was low (Fig. 4(a)), giving too low an α value leading to an insufficient peak stress (σ^*) for the translamellar fracture, the interlamellar cleavage occurs with the help of the mode-II component of applied stress (σ_∞). The above two viewpoints are strongly complementary, not competitive.

In summary, with regard to the stress concentration associated with a dislocation pile-up against an interface, the role of energetic barriers estimated on the basis of linear elasticity is relatively unimportant as compared to that of kinetics of the dislocation reaction resulting from the leading dislocation. In other words, how effectively the reaction products move away from the site of intersection is far more crucial to whether or not the following dislocations can be incorporated into the interface. Further research is needed to understand effects of temperature and strain rate on the climb mobility of interfacial dislocations that influence the intrinsic brittle-to-ductile transition behavior.

Acknowledgments

The author would like to thank Dr. G. Sauthoff of MPI für Eisenforschung and Prof. H. Mecking of TUHH for helpful discussions and their staff members for kind assistance during the course of this work.

References

1. M. Yamaguchi and H. Inui, "TiAl Compounds for Structural Applications," Structural Intermetallics, eds., R. Darolia, J. J. Lewandowski, C. T. Liu, P. L. Martin, D. B. Miracle, and M. V. Nathal, (TMS Publ., Warrendale, PA, 1993), 127-142.
2. F. Appel and R. Wagner, "The Structure and Stress State of Lamellar Interfaces in Two-Phase Titanium Aluminides," Interfacial Control of Electrical, Chemical, and Mechanical Properties, eds. S. P. Murarka, K. Rose, T. Ohmi, and T. Seidel, (MRS Symp. Proc. Vol. 318, MRS, Pittsburgh, PA, 1994), 691-696.
3. S-C. Huang and E. L. Hall, "Plastic Deformation and Fracture of Binary TiAl-Base Alloys," Metall. Trans., A22 (1991), 427-439.
4. Y-W. Kim and D. M. Dimiduk, "Progress in the Understanding of Gamma Titanium Aluminides," J. of Metals, 43, 8 (1991), 40-47.
5. P. M. Hazzledine and B. K. Kad, "Yield and Fracture of Lamellar γ/α_2 TiAl Alloys," Mater. Sci. and Eng. (in press).
6. T. Nakano, A. Yokoyama, and Y. Umakoshi, "Effect of Nb Addition on the Plastic Behavior of TiAl Crystals containing Oriented Lamellae," Scr. Metall. Mater., 27 (1992), 1253-1258.
7. M. H. Yoo, J. Zou, and C. L. Fu, "Mechanistic Modeling of Deformation and Fracture Behavior in TiAl and Ti_3Al ," Mater. Sci. and Eng. (in press).
8. M. H. Oh, H. Inui, M. Misaki, and M. Yamaguchi, "Environmental Effects on the Room Temperature Ductility of PST Crystals of TiAl," Acta Metall. Mater., 41 (1993), 1939-1949.
9. J. D. Eshelby, F. C. Frank, and F.R.N. Nabarro, Phil. Mag., 42 (1951), 531.
10. M. H. Yoo and A. H. King, "Intergranular Fracture by Slip/Grain Boundary Interaction," Metall. Trans. A, 21 (1990), 2431-2436.
11. Y. T. Chou and J.C.M. Li, Mathematical Theory of Dislocations, ed. T. Mura, (ASME, New York, 1969), 116.
12. H. Tada, P. Paris, and G. Irwin, The Stress Analysis of Cracks Handbook, (Del Research Corp., 1985).
13. M. H. Yoo and H. Trinkaus, "Interaction of Slip with Grain Boundary and Its Role in Cavity Nucleation," Acta Metall. Mater., 34 (1986), 2381-2390.
14. A. G. Evans, J. R. Rice, and J. P. Hirth, "Suppression of Cavity Formation in Ceramics: Prospects for Superplasticity," J. Am. Ceram. Soc., 63 (1980), 368-375.
15. C. L. Fu and M. H. Yoo, "Elastic Constants, Fault Energies, and Dislocation Reactions in TiAl: A First-Principles Total-Energy Investigation," Phil. Mag. Lett., 62 (1990), 159-165.
16. M. H. Yoo and C. L. Fu, "Cleavage Fracture of Ordered Intermetallic Alloys," Mater. Sci. Eng. A, 153 (1992), 470-478.
17. M. H. Yoo and A. H. King, "Slip, Twinning, and Fracture at a Grain Boundary in the $L1_2$ Ordered Structure -- A $\Sigma = 9$ Tilt Boundary," J. Mater. Res., 3 (1988), 848-855.
18. S. Rao, C. Woodward, J. Simmons, and D. M. Dimiduk, "Core Structure and Mobility of $<10\bar{1}$ Dislocations in $L1_0$ TiAl," High-Temperature Ordered Intermetallic Alloys-VI, eds. J. A. Horton, I. Baker, S. Hanada, R. D. Noebe, and D. F. Schwartz (MRS Symp. Proc., MRS, Pittsburgh, PA, 1995), in press.
19. A. Courret, S. Farenc, D. Caillard, and A. Coujou, "Twin Nucleation, Propagation and Growth in TiAl," Twinning in Advanced Materials, eds. M. H. Yoo and M. Wuttig (TMS Symp. Proc., TMS, Warrendale, PA, 1994), 361-374.